Princeton Plasma Physics Laboratory

PPPL- 4288

PPPL- 4288

Anode Sheath Switching in a Carbon Nanotube Arc Plasma

Abe Fetterman, Yevgeny Raitses, and Michael Keidar

April 2008

Prepared for the U.S. Department of Energy under Contract DE-AC02-76CH03073.

Princeton Plasma Physics Laboratory
Report Disclaimers

Full Legal Disclaimer

Trademark Disclaimer

PPPL Report Availability

Princeton Plasma Physics Laboratory:

http://www.pppl.gov/techreports.cfm

Office of Scientific and Technical Information (OSTI):

http://www.osti.gov/bridge

Related Links:

U.S. Department of Energy

Office of Scientific and Technical Information

Fusion Links

Anode sheath switching in a carbon nanotube arc plasma

Abe Fetterman, Yevgeny Raitses, and Michael Keidar

February 8, 2008

Abstract

The anode ablation rate is investigated as a function of anode diameter for a carbon nanotube arc plasma. It is found that anomalously high ablation occurs for small anode diameters. This result is explained by the formation of a positive anode sheath. The increased ablation rate due to this positive anode sheath could imply greater production rate for carbon nanotubes.

1 Introduction

The discovery of single-walled carbon nanotubes in 1993 [1, 2, 3, 4] sparked significant interest in the scientific community because of the diverse properties of this new material. Nanotubes have been considered for hydrogen storage, capacitor construction, flat-panel displays, material strengthening, micromotors, and many other applications [5]. Nanotubes can be produced in many ways [6], but the atmospheric pressure helium arc discharge remains one of the simplest methods for producing large quantities of single-walled carbon nanotubes (CNTs) [7]. This method continues to see innovation in both production volume and quality of nanotube output [8, 9, 10]. In such arc discharges, anode phenomena play an important role in nanotube formation. Anode ablation produces carbon atoms that are ionized to form the plasma, which will eventually condense into CNTs.

A number of previous studies focused on anode phenomena due to spot formation in either vacuum arcs and furnaces, or in high current regimes (> 1000 A) [11, 12]. The anode process has also been studied theoretically in lower pressure regimes with longer arcs [13]. Surprisingly, the anode process of arc discharges for nanotube applications has received little attention. Keidar et al [14, 15] have developed a rigorous description of this ablation process in the appropriate regime, as long as discharge parameters are known. In this model, the near-anode sheath is assumed to be electron repelling (a so-called "negative anode sheath" or "negative anode fall"). In a negative anode sheath, the plasma potential at the boundary of the anode sheath is higher than the anode potential [16, 17].

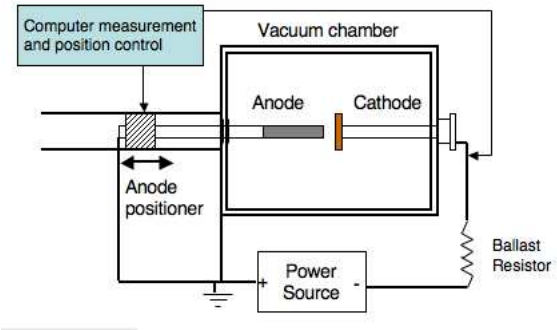

Figure 1: A diagram of the setup used for this experiment.

Negative and positive anode sheath regimes, and their dependence on discharge parameters, electrode geometry, and configuration are known for different types of gas discharges (e.g. glow discharges, low pressure arcs, etc) [16, 17, 18], but not for short length carbon arcs used in nanotube production. In the Keidar et al model [14, 15], the negative anode sheath governs the anode ablation and, consequently, defines the carbon source in CNT production. A consequence of the negative anode sheath is that power deposition to the anode will be dependent primarily on the plasma temperature, density, and surface area. Because of this, one expects ablation to be maximized for an anode diameter equal to the arc diameter, which maximizes power deposition (surface area), and minimizes cooling along the anode. In the present work, we show experimentally that by decreasing the anode diameter below a certain threshold diameter, the ablation rate can be increased. We explain this behavior by the transition of the anode sheath from negative to positive (electron attractive), leading to enhanced power deposition on the anode.

2 Experimental Setup

The experimental setup (Fig. 1) consists of a rod shaped graphite anode, and a disk shaped copper cathode. To test the predicted scaling of the ablation rate, we used graphite anodes that varied in diameter from 0.4 cm to 1.25 cm, and in length from 5 cm to to 15 cm. The copper cathode has a substantially larger diameter (5 cm) than the anode, so that it is expected to make contact with the entire arc. The experiment was carried out in a helium atmosphere at 600 torr, in a 10 inch four-way cross. The chamber was pumped down to ten millitorr before a helium gas was introduced to the chamber.

The graphite anode was mounted on a motorized linear positioner that was computer controlled. A linear potentiometer attached to the positioner was used to monitor the anode position with respect to the cathode. The arc voltage and current, as well as the potentiomter output voltage, were recorded by a PC-based

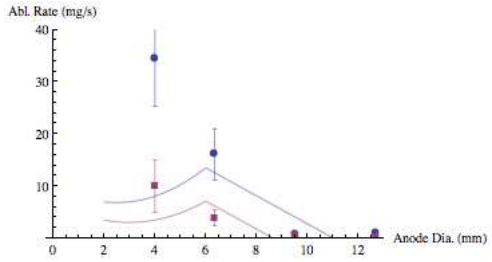

Figure 2: Ablation data and predicted curves. Blue line is theory for 70 A, red line for 50 A. Blue circles are data for 70 A, and red squares are data for 50 A.

data aquisition and control system. A computerized negative feedback between the arc voltage and the interelectrode gap was used to maintain constant voltage, and thus a constant gap between the anode and the cathode of about 0.2 cm. To initiate the arc discharge, the graphite anode was brought into contact with the copper cathode. Once the arc is struck, the interelectrode gap is increased at a moderate speed (slow enough that the arc is approximately steady state, but fast enough that the ablation is not significant).

The ablation rate was determined by running the arc in a steady state at constant voltage and current. After running for an allotted time (12 seconds to 8 minutes) the anode was removed, measured and weighed. This process was repeated at least three times for each ande, and also two to three times for different anode samples of the same diameter. The error bars for the ablation rate were estimated using the standard deviation of multiple measurements, weighted by the amount of time the arc was running for that measurement.

3 Results and discussion

Figure 2 compares experimental and theoretical ablation rates. The theoretical values were obtained using the zero-order model presented in Section 4.

One finds that for anode diameters larger than about 8 mm, the ablation remains small but constant. We suspect that a colder plasma is formed, with larger sheath regions without local thermodynamic equilibrium. This would decrease the ability of the anode to cool the plasma, and allow stable operation of the arc. This is supported by the measurements of Ostrogorsky et al, who found a decreasing plasma temperature with increasing anode size [19]

The most notable feature of the results is that at low anode diameter (below 6 mm), ablation is significantly larger than the predicted values. We suggest that this phenomenon is due to a change in the behavior of the anode sheath. At large diameters, the anode sheath voltage is negative, as would be predicted. Because the thermal electron flux is greater than the current flux, the electrons are repelled from the anode surface by a negative voltage. When the anode diameter becomes small, though, the opposite effect occurs. The lines of current

which are spread uniformally across the arc must converge to reach the anode. This requires a positive anode sheath voltage.

It is possible to estimate this anode sheath voltage by making some assumptions about the plasma. The resistance across the plasma may be written as $\pi r_0^2 \ell \bar{\eta}$, where $\bar{\eta}$ is the average resistivity in the plasma. Then the change in the resistance of the plasma per change in plasma length ($d/d\ell$) is:

$$\frac{dR}{d\ell} = \pi r_0^2 \bar{\eta} \left(1 + \frac{2\ell}{r_0} \frac{dr_0}{d\ell} + \frac{\ell}{\bar{\eta}} \frac{d\bar{\eta}}{d\ell} \right) \tag{1}$$

If we suppose that the radius and resistivity do not change significantly for small changes in the arc length, then we can calculate the plasma resistance knowing the arc length and change in resistance per change in length. By using the voltage and current data aquired for the calibration, we can produce a measure of the resistance of the arc as a function of the arc length.

Combining the measurement of the plasma voltage (arc resistance times current) with the total measured voltage, we can find the voltage in the combined electrode sheaths. The voltage in the cathodic sheath is essentially constant for a given cathode material, current, and incoming ion species [20], so that this is, up to a constant, indicitive of the anode sheath voltage. The results of this calculation are shown in Figure 3.

Several features of these graphs are interesting. The electrode voltage (Figure 3d-f) seems to reach a minimum at an anode diameter near 10 mm. However, for the large diameter anodes the error bars grow to be large. In this case, the arc diameter is probably smaller than the anode diameter, and the location of the arc attachment may be varying across experiments, effecting the measurement of the plasma voltage. The arc diameter and attachement may vary due to an uneven anode surface caused by ablation, or by spot formation processes similar to those recently studied in thermionic cathodes [21]. There is also strange behavior of the 6.25 mm diameter arc at 50 A. This behavior is repeatable for the single case, but since the effect does not occur over other diameters or currents, the data offers no clear explanation. One trend in Figure 3d-f that does seem clear is that the electrode voltage increases as the anode diameter is decreased from 10 mm (with the exception of the 6.25 mm diameter anode at 50 A). This is especially the most interesting trend combined with our observation of high ablation for these low diameter anodes.

We will focus on this rise in the electrode potential with decreasing anode diameter. Because the cathode sheath potential is nearly constant, as mentioned earlier, we may assume that this potential rise is increasing in the anode sheath. It can be seen that this is necessary to explain the data. Results from the model (which excludes an anode sheath potential) suggest that the 6 mm diameter anode being driven with 70 Amperes has $T_e = 0.6\,\mathrm{eV}$ and $n_e = 10^{14}\mathrm{cm}^{-3}$. The thermal flux $J = \frac{1}{4} n_e v_{Te}$ gives a current of only 36 Amperes, insufficient for the required 70 Amperes of current.

The increased voltage can increase the current in two ways. One way is by increasing the ionization of carbon atoms inside the sheath, leading to a an

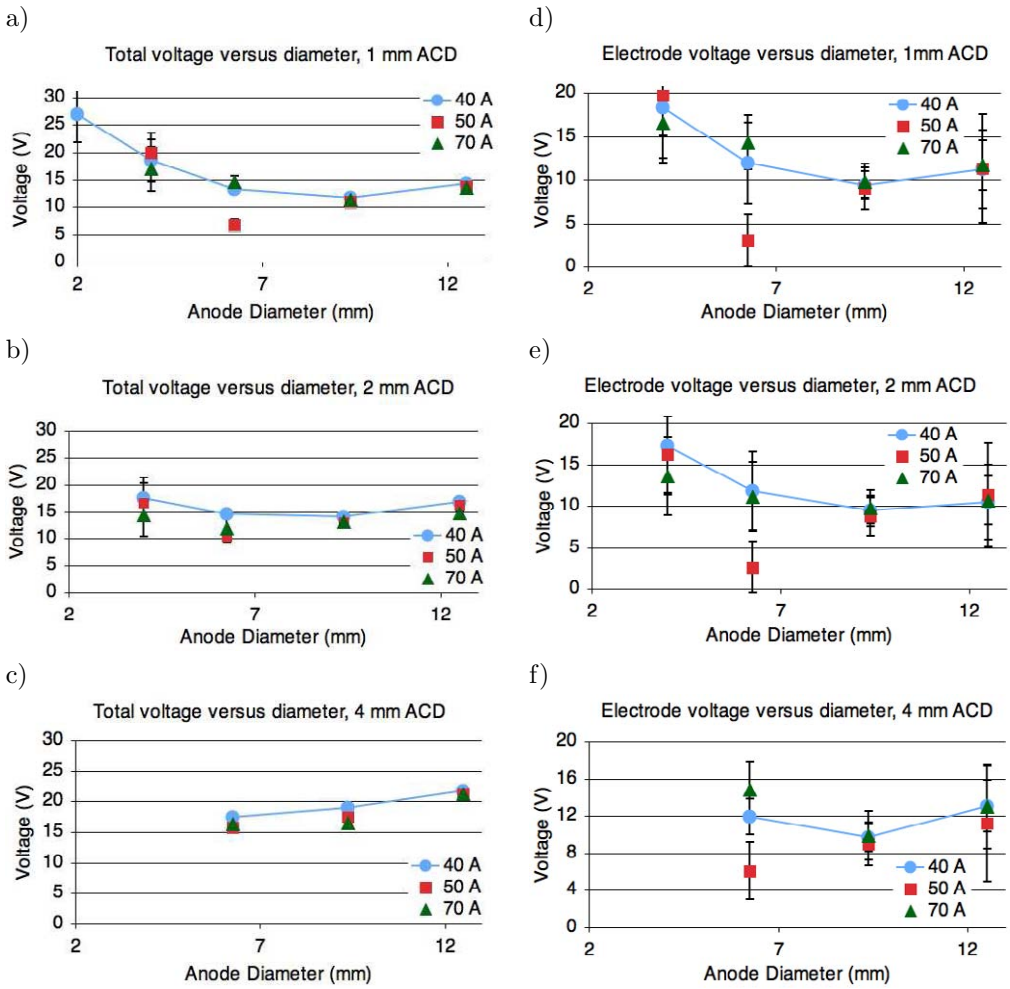

Figure 3: The total measured voltage (a-c) and the combined voltage of the electrodes (d-f), as calculated by removing the estimated plasma voltage. The results are shown for an anode-cathode distance (ACD) of 1 mm, 2 mm, and 4 mm.

increased flow of positive ions away from the electrode. The other mechanism is to reshape the plasma in the near-anode region into a cone converging on the anode. This effectively increases the area of the anode so that it can capture a larger amount of electron flux. It is difficult to determine which of these plays a more important role. Theory on the anode sheath voltage due to convergence is especially complicated due to the short length of our arc, as well as its free burning, high-pressure nature [22].

4 Anode energy balance

In order to demonstrate how the experimental results differ from the expected scaling, we will calculate numerical estimates for the ablation using a simple anode energy balance. Energy comes to the anode by the electron heat flux from the plasma (Q_e) and by thermal conduction from the plasma (Q_{He}). It leaves the anode through carbon ablation (Q_C) and thermal conduction along the anode (Q_a) [15]:

$$Q_e + Q_{He} = Q_C + Q_a. \tag{2}$$

Electron power The power deposited by the electrons is given by:

$$Q_e = (I/e)\left(2T_e + \phi_e\right), \tag{3}$$

where I is the total arc current, e is the electron charge, T_e is the plasma electron temperature, and ϕ_e is the electron work function.

Heat conduction The heat conduction from the arc is:

$$Q_{He} = \frac{A_a}{L_a}\int_{T_a}^{T_{He}} K\, dT, \tag{4}$$

where $A_a^\star$ is the anode surface area *exposed to the plasma*, T_{He} is the plasma helium temperature, and T_a is the anode temperature. If the arc plasma area is A_p, then $A_a^\star$ is the minimum of A_a and A_p. L_a is the anode sheath scale length, taken to be twice the Helium mean free path [23]. K is the thermal conductivity of Helium (considered the primary heat conductor). An expression for the thermal conductivity may be found by treating Helium as an ideal gas [24]:

$$K\left(T\right) = \frac{1}{2}\frac{\sqrt{T/m_{He}}}{\pi r_{He}^2}, \tag{5}$$

where r_{He} is the radius of a helium atom and m_{He} is the Helium atomic mass. We take the scale of the anode sheath to be two Helium mean free paths, $L_a = 2v_{THe}/\nu_{He}$ [23].

Carbon ablation Carbon ablation leads to the cooling:

$$Q_C = (\phi_C + C_p T_a)\,\frac{\dot{m}_a}{m_C}. \tag{6}$$

ϕ_C is the heat of evaporation of carbon, and C_p is the heat capacity of graphite. $\dot{m}_a$ is the rate of change of the anode mass, and m_C is the mass of a carbon atom.

Anode cooling The anode is a long conductive rod that is cooled by its contact with the helium background gas. If we take the background gas thermal conductivity given in Eq (5) and constant graphite thermal conductivity $k_C = 85W/m \cdot K$, we find the cooling by the helium per unit length to be:

$$\frac{dW}{dx} = \pi r_a^2 k_C \frac{d^2T}{dx^2} = 2\pi \int_0^T K\,dT, \tag{7}$$

where r_a is the anode radius. Solving this at the surface, for $T = T_a$:

$$Q_a = k_C A_a \left(\frac{8}{15\sqrt{m_{He}} r_{He}^2 k_c A_a}\right)^{1/2} T_a^{5/4}, \tag{8}$$

and here A_a is the total anode area.

Remaining variables We are now able to solve for the ablation rate, $\dot{m}_a$, using the anode area A_a, the cross-sectional area of the arc A_p, the anode temperature T_a, and arc Helium temperature T_{He}. The arc radius is estimated to be near 3 mm [25], the anode temperature is measured to be near 3000 K [19]. For a current of 50 A, we use a Helium temperature of 6000 K from Ostrogorsky et al, whose experiment ran at 42 A. For theory at a current of 70 A, an approximate Helium temperature of 7000 K was used from Marcovic et al, whose experiments ran at 100 A [26].

The results appear in figure 2. Below 6 mm, there is a quadratic rise in the ablation rate, due to the increasing anode surface area exposed to the plasma ($\propto \pi r_a^2$). One sees the expected linear dropoff in ablation rate above 6 mm, due to the increase in the anode surface area available to cooling ($\propto 2\pi r_a$).

5 Conclusion

Arc discharge experiments were conducted with graphite anodes of different diameters, with a focus on the effect on the carbon mass ablation rate. The expected result of a peak ablation rate where the anode diameter equals the plasma diameter was not found. Instead, the ablation rate increased significantly for small anode sizes. We have shown that this is likely due to the formation of a positive anode sheath.

Because the anode provides the plasma ions, and eventually the raw material for carbon nanotube production, understanding of the anode ablation is critical

to understanding the arc operation as a whole. As the Helium electric arc technique for producing SWCNTs continues to be developed, further analysis of the anode region and anode phenomena are necessary to predict and explain arc behavior. This paper shows that there is much left to be known about anode behavior in this particular arc.

Acknowledgments

The authors thank Drs. Stewart Zweben, Phillip Efthimion, and Nathaniel Fisch for their encouraging support of this work. Thanks also to Dick Yager for his technical assistance with the experiment.

References

[1] Marc Monthioux and Vladimir L. Kuznetsov. Who should be given credit for the discovery of carbon nanotubes? *Carbon*, 44:1621–1623, 2006.

[2] Sumio Iijima. Helical microtubules of graphitic carbon. *Nature*, 354:56–58, 1991.

[3] Sumio Iijima and Toshinari Ichihashi. Single-shell carbon nanotubes of 1-nm diameter. *Nature*, 363:603 – 605, 1993.

[4] D. S. Bethune, C. H. Klang, M. S. de Vries, G. Gorman, R. Savoy, J. Vazquez, and R. Beyers. Cobalt-catalysed growth of carbon nanotubes with single-atomic-layer walls. *Nature*, 363:605 – 607, 1993.

[5] Ray H. Baughman, Anvar A. Zakhidov, and Walt A. de Heer. Carbon nanotubes–the route toward applications. *Science*, 297:787–792, 2002.

[6] ET Thostenson, ZF Ren, and TW Chou. Advances in the science and technology of carbon nanotubes and their composites: a review. *Composites Science and Technology*, 61:1899–1912, 2001.

[7] C. Journet, W. K. Maser, P. Bernier, A. Loiseau, M. Lamy de la Chapelle, S. Lefrant, P. Deniard, R. Lee, and J. E. Fischer. Large-scale production of single-walled carbon nanotubes by the electric-arc technique. *Nature*, 388:756–758, 1997.

[8] Feng Du, Yanfeng Ma, Xin Lv, Yi Huang, Feifei Li, and Yongsheng Chen. The synthesis of single-walled carbon nanotubes with controlled length and bundle size using the electric arc method. *Carbon*, 44, 2006.

[9] S.P. Doherty, D.B. Buchholz, and R.P.H. Chang. Semi-continuous production of multiwalled carbon nanotubes using magnetic field assisted arc furnace. *Carbon*, 44, 2006.

[10] A Mansour, M Razafinimanana, M Monthioux, M Pacheco, and A Gleizes. A significant improvement of both yield and purity during swcnt synthesis via the electric arc process. *Carbon*, pages 1651–1661, 2007.

[11] A Lefort, M J Parizet, S E El-Fassi, and M Abbaoui. Erosion of graphite electrodes. *J. Phys. D: Appl. Phys*, 26:1239–1243, 1993.

[12] Isak I. Beilis. Anode spot vacuum arc model: Graphite anode. *IEEE Transactions on Components and Packaging Technologies*, 23:334–340, 2000.

[13] N. I. Alekseyev and G. A. Dyuzhev. Arc discharge with a vaporizable anode: Why is the fullerene formation process affected by the kind of buffer gas? *Technical Physics*, 46:1247–1255, 2001.

[14] Michael Keidar, Jing Fan, Iain D. Boyd, and Isak I Beilis. Vaporization of heated materials into discharge plamas. *Journal of Applied Physics*, 89:3095–3098, 2001.

[15] M. Keidar, A.M. Waas, Y. Raitses, and E.I. Waldorff. Modeling of the anodic arc discharge and conditions for single-wall carbon nanotube growth. *Journal of Nanoscience and Nanotechnology*, 6:1309–1314, 2006.

[16] I. Langmuir and H. M. Mott-Smith. *General Electric Review*, 27:449, 538, 616, 761, 810, 1924.

[17] B. N. Kliarfeld and N. A. Neretina. Anode region in a low-pressure gas discharge: 1. effect of anode shape on sign and magnitude of the anode fall. *Soviet Physics: Technical Physics*, 3:271, 1958.

[18] Leonid A. Dorf, Y Raitses, and N J Fisch. Anode sheath in hall thrusters. *Applied Physics Letters*, 83:2040, 2003.

[19] A. G. Ostrogorsky and C. Marin. Heat transfer during production of carbon nanotubes by the electric-arc process. *Heat Mass Transfer*, 42, 2006.

[20] Yuri P. Raizer. *Gas Discharge Physics*. Springer-Verlag, New York, 1991.

[21] MS Benilov. Stability of direct current transfer to thermionic cathodes: I. analytical theory. *Journal of Physics D: Applied Physics*, 40:1376–1393, 2007.

[22] Max F. Hoyaux. *Arc Physics*. Springer-Verlag, New York, 1968.

[23] Valerian A Nemchinsky. Anode layer in a high-current arc in atmospheric pressure nitrogen. *Journal of Physics D: Applied Physics*, 38:4082–4089, 2005.

[24] Earle H. Kennard. *Kinetic Theory of Gases*. McGraw-Hill, New York, 1938.

[25] H Lange, K Saidane, M Razafinimanana, and A Gleizes. Temperatures and c2 column densities in a carbon arc plasma. *Journal of Physics D: Applied Physics*, 32:1024–1030, 1999.

[26] Z. Markovic, B. Todorovic-Markovic, M. Marinkovic, and T. Nenadovic. Temperature measurement of carbon arc plasma in helium. *Carbon*, 41:369–371, 2003.

The Princeton Plasma Physics Laboratory is operated
by Princeton University under contract
with the U.S. Department of Energy.

Information Services
Princeton Plasma Physics Laboratory
P.O. Box 451
Princeton, NJ 08543

Phone: 609-243-2750
Fax: 609-243-2751
e-mail: pppl_info@pppl.gov
Internet Address: http://www.pppl.gov